Transport via coupled states in a C_{60} peapod quantum dot

Anders Eliasen,[1] Jens Paaske,[1,*] Karsten Flensberg,[1] Sebastian Smerat,[2,3,4] Martin Leijnse,[1,3,4] Maarten R. Wegewijs,[5,3,4] Henrik I. Jørgensen,[1] Marc Monthioux,[6] and Jesper Nygård[1]

[1]*Niels Bohr Institute & Nano-Science Center, University of Copenhagen, Universitetsparken 5, 2100 Copenhagen Ø, Denmark*

[2]*Ludwig-Maximilians-Universität München, Physics Department, Arnold Sommerfeld Center for Theoretical Physics, and Center for NanoScience, Ludwig-Maximilians-Universität München, D-80333 München, Germany*

[3]*Institut für Theoretische Physik A, RWTH Aachen, 52056 Aachen, Germany*

[4]*JARA-Fundamentals of Future Information Technology*

[5]*Institut für Festkörperforschung, Forschungszentrum Jülich, 524 25 Jülich, Germany*

[6]*Centre d'Elaboration des Matériaux et d'Etudes Structurales (CEMES), UPR A-8011 CNRS, B.P. 94347, 29 Rue Jeanne Marvig, F-31055 Toulouse Cedex 4, France*

(Received 2 February 2010; revised manuscript received 26 March 2010; published 15 April 2010)

We have measured systematic repetitions of avoided crossings in low-temperature three-terminal transport through a carbon nanotube with encapsulated C_{60} molecules. We show that this is a general effect of the hybridization of a host quantum dot with an impurity. The well-defined nanotube allows identification of the properties of the impurity, which we suggest to be a chain of C_{60} molecules inside the nanotube. This electronic coupling between the two subsystems opens the interesting and potentially useful possibility of contacting the encapsulated molecules via the tube.

DOI: 10.1103/PhysRevB.81.155431 PACS number(s): 73.22.−f, 73.61.Wp, 73.63.Fg

I. INTRODUCTION

Peapod systems represent a next step in complexity of carbon-based electronics, departing from the well-characterized single-walled nanotube system. Since the advent[1] of these single-walled carbon nanotubes (CNTs) filled with C_{60} molecules (or other fullerenes), there has been an ongoing experimental effort to clarify the modification of the electronic properties of the CNT. In particular, the hybridization of the C_{60} molecules with the CNT electronic states is of importance for addressing the molecular scale "peas" via the CNT, for instance using spin-exchange processes. More generally, the interaction of quantum dot systems of different nature and the associated transport signatures are of broad interest. Band structure calculations[2–7] have suggested that the hybridization between the CNT and the encapsulated C_{60} molecules could lead to an extra band crossing the Fermi level in a metallic peapod, depending on tube chirality, but the experimental evidence for such mixing between the two subsystems remains ambiguous.

Since the first transmission electron microscopy images of the encapsulated molecules,[1] scanning tunneling microscopy (STM) has been used to probe the electronic states of a single peapod, showing that they were indeed different from those of an empty CNT.[8] These STM data of Hornbaker *et al.*[8] were rationalized in terms of a semiempirical model invoking a coupling between the CNT π-orbitals and the t_{1u} states of a C_{60} of the order of 1.25 eV, indicative of substantial hybridization of the two subsystems. DFT results of Lu *et al.*[4] predicted one order of magnitude smaller hybridization. Subsequent photoemission studies[9] even showed no evidence for hybridization between C_{60} molecules and tube.

Also low-temperature transport measurements of peapods prepared as three-terminal quantum dots have been performed,[10–13] but the results remain inconclusive. Refs. 10 and 11 find no evidence for electronic structures deviating from that of empty CNT quantum dots, whereas Refs. 12 and 13 showed irregular diamond-structures which were suggested to derive from the encapsulated C_{60} system. Since, at present, simultaneous imaging and transport measurements are not possible, these experiments may have probed peapods with rather different electronic structure. For a consistent picture to emerge, more experiments on high-quality peapod samples are clearly necessary. Thus the question still remains whether the peapod system can provide new, interesting and potentially useful functionality for nanoelectronic circuitry?

We report a new set of detailed low-temperature transport measurements for a peapod quantum dot device in the weakly coupled Coulomb blockade regime. As in Refs. 10 and 11 we observe well-defined Coulomb diamonds reflecting the discrete charging of the CNT. In contrast to Refs. 10 and 11 and to similar measurements on empty CNT quantum dots, we observe a systematic repetition of avoided crossings in a gate-range corresponding to some 400 consecutive charge-states. This systematic feature results from a weak hybridization with a weakly gated localized orbital, as detailed comparisons with master equation calculations show. We tentatively propose these signatures to relate to a short chain of C_{60}-molecules inside the CNT, residing close to one electrode.

II. EXPERIMENTAL RESULTS

The single-walled C_{60} peapods of purity grade 90–95 % (see Ref. 10 for synthesis details), were suspended in dichloroethane by sonification and dispersed in the form of droplets onto an isolating SiO_2 layer of thickness 500 nm, thermally grown on top of a highly doped silicon substrate. By use of atomic force microscopy imaging, individual tubes were identified and then contacted by evaporated source and drain Ti/Au-electrodes (25 nm/25 nm) using e-beam lithography.

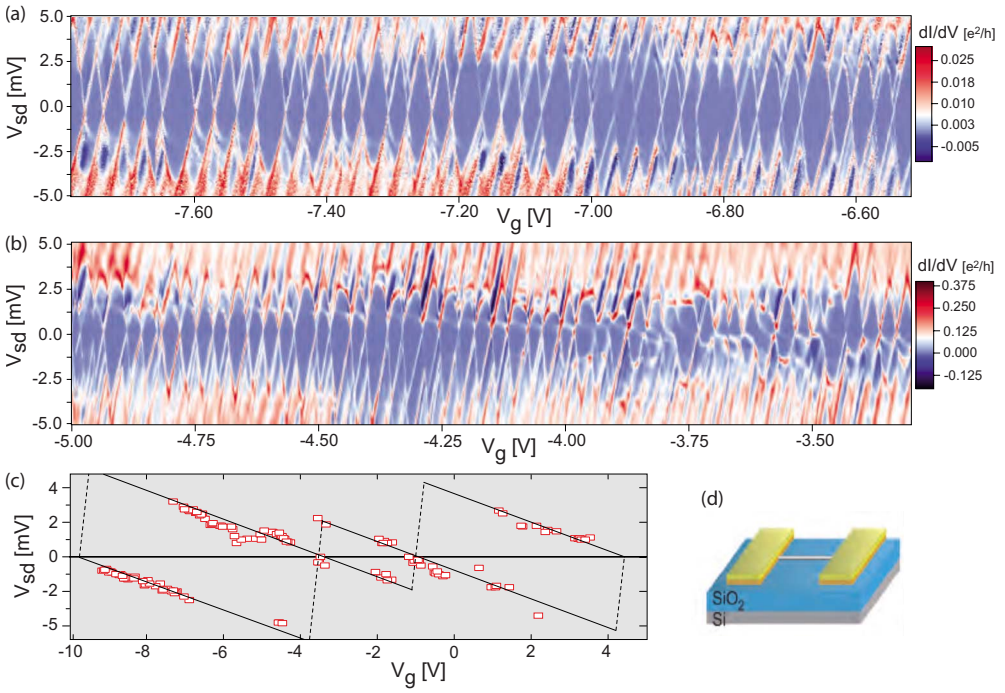

FIG. 1. (Color online) (a) and (b) Stability diagram, i.e., conductance (dI/dV_{sd}) as a function of source-drain bias (V_{sd}) and gate voltage (V_g) at 300 mK, showing a regular Coulomb blockade diamond pattern with four-electron shell structure throughout the measured gate range. Diamonds are perturbed by a weakly gate-dependent feature superimposed on the entire structure. (c) Observed avoided crossings over the entire gate-range (red rectangles). Black lines are guides to the eye, outlining the edges of the "impurity diamond." (d) Sketch of the peapod quantum dot device.

The device layout, including the electrodes separated by $L \approx 600$ nm, is shown schematically in Fig. 1(d).

We have performed electronic transport measurements down to 300 mK in a ^{3}He cryostat, using standard lock-in techniques (ac source-drain voltage 50 μV RMS). Sweeping the gate-voltage V_g and measuring the linear conductance, we observe Coulomb blockade peaks in metallic peapod samples.[10] Here we concentrate on a single sample exhibiting highly regular Coulomb blockade peaks in the region $-10\ \text{V} < V_g < 5\ \text{V}$, representative gate ranges being shown in Figs. 1(a) and 1(b). We observe a clear four-electron shell structure similar to that of empty CNTs.[14–16]

Unlike the device measured in Ref. 13, which also exhibited traces of a four-electron shell, there is no reason to believe that the device studied here has been accidentally partitioned into smaller subsystems. In Ref. 13, the presence of distinct gate-voltage regions with rather different, and surprisingly large diamond sizes ($E_{add} \simeq 10-20$ meV for a peapod of length 500 nm), was interpreted as the tube being separated into two or more smaller "dots."

Having established the salient quantum dot features of these transport data presented in Figs. 1(a) and 1(b) as essentially CNT-like, one notices a distinct perturbation of the entire stability diagram: a very weakly gate-dependent resonance line passes through the diamonds at positive and/or negative bias, depending on the gate voltage, and anticrosses with the edges of the CNT Coulomb diamonds. Figure 1(c) shows the gate and bias positions of these avoided crossings over the entire gate-range where such features were observed. The weakly gate-dependent resonance and the associated avoided crossings are seen more clearly in Fig. 2(a), which zooms in on a representative gate range in Fig. 1(b). Due to the weak gate-dependence this line might have been assigned to inelastic cotunneling.[19] This would, however, be inconsistent with the observed avoided crossings with one

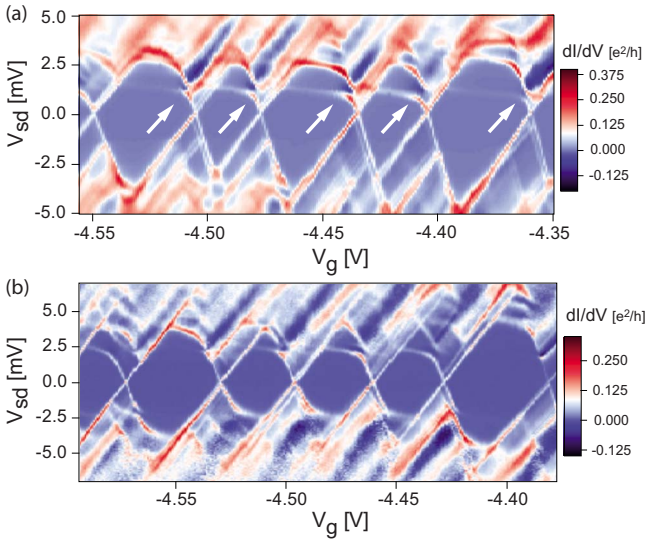

FIG. 2. (Color online) (a) Zoom in on a representative range of gate-voltages in Fig. 1(b). At positive bias we observe a series of avoided crossings with a line of much lower gate coupling than the main diamond edges. (b) The same device after suspension. Avoided crossings are seen at both negative and positive bias in the displayed gate range.

side of the CNT diamond edges. Furthermore, the weakly gate-dependent resonance does not occur symmetrically at the same energy at positive and negative bias, as inelastic cotunneling resonances do, and for most gate voltages it is only present either at positive or negative bias-voltage and strongly perturbs the single-electron tunneling (SET) region on the corresponding bias side, showing broad regions of negative/positive differential conductance (NDC/PDC).

As will be further substantiated below, all of these observations are instead consistent with SET through a state which: (i) is much weaker coupled to the back gate than are the levels of the CNT; (ii) hybridizes with the levels of the CNT; (iii) has a significant capacitive and tunnel coupling only to the source lead. We refer to this state as an "impurity orbital" to emphasize the general nature of the transport effect in the following analysis. After this we will argue that the impurity consists of a short chain of C_{60} molecules inside the tube.

III. MODELING

Independent of the precise origin of the impurity we can extract detailed information about this state and its coupling to the CNT. Figure 3(a) shows the result of model calculations, reproducing the transport features in the central part of Fig. 2(a). We model the CNT plus impurity state as sketched in Fig. 3(b), including only the lowest two subbands of the CNT due to the large level-spacing $\Delta E \sim E_C$. The other parameters of the constant interaction model[16,17] are extracted from the experiment: $E_C=2.9$ meV (charging energy), $\delta=1.2$ meV (subband splitting), and $dU=0$ meV (excess Coulomb energy). The exchange coupling, J, is difficult to extract from the data since it can only be observed in transitions involving excited states. We therefore take $J=0$ meV, having verified that other values do not qualitatively change the result.

The avoided crossings in the experimental data indicate that both CNT orbitals (subbands 1 and 2) hybridize significantly with the impurity orbital. Due to the different gate and bias couplings of the CNT and impurity states (see below), the many-body peapod model (CNT plus impurity plus hopping) has to be diagonalized exactly at each gate- and bias-voltage point. Standard master equations[18] (lowest order perturbation theory in the tunnel coupling to the leads) then suffice to explain all the features.

In the experimental setup the voltage is applied only to the source, while the drain lead is grounded, $V_{sd}=V_s \propto -|e|\mu_s$, where $-|e|$ is the electron charge and μ_s the chemical potential of the source electrode. The voltage dependence of the energy ϵ_m of orbital $m=1,2$ (CNT) and $m=i$ (impurity), is then given by

$$\epsilon_m \propto -|e|\alpha_g^m V_g - |e|\alpha_s^m V_{sd}, \tag{1}$$

where $\alpha_k^m = C_k^m / C^m$, with $C^m = C_s^m + C_d^m + C_g^m$ being the sum of the capacitances to the source, drain and gate electrodes. Figure 3(c) shows a sketch of a small part of a diamond with one avoided crossing and indicates how to read off the gate- and bias-couplings far from the avoided crossing, where there is little mixing between the CNT and impurity states.

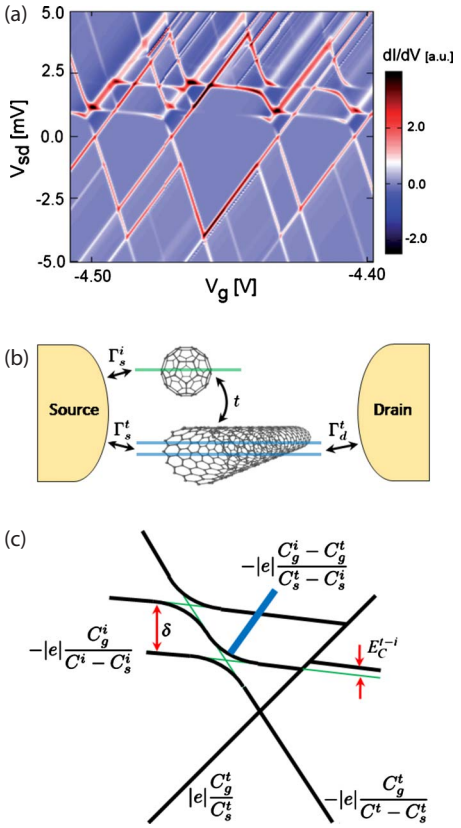

FIG. 3. (Color online) (a) Calculated stability diagram showing dI/dV_{sd} as a function of source-drain bias (V_{sd}) and gate-voltage (V_g) for a gate-voltage range corresponding to the three central diamonds in Fig. 2(a). In the calculation we use the experimental temperature $T=300$ mK, but neglect tunnel broadening. Therefore all resonances are somewhat sharper than in the experiment. (b) Model system used in the calculation. The impurity level hybridizes with both CNT subbands (amplitude t), but is only tunnel coupled to the source (rate Γ_i^s). Both CNT subbands are coupled with the same rate to source and drain ($\Gamma_t^s = \Gamma_t^d$). (c) Sketch of avoided crossings. The capacitances associated with the tube and impurity can be read off from the slope of the resonance lines far from the avoided crossing.

For the CNT (regular pattern of Coulomb diamonds) we find $\alpha_g^{1(2)}=0.104$, $\alpha_s^{1(2)}=0.298$ (the same for both subbands). Although the impurity resonance (weakly gate-dependent line) crosses the zero-bias line, e.g., at around $V_g=-3.75$ V ["impurity degeneracy point," see Fig. 1(b)], only one side of the "impurity diamond" (the drain-resonance) can be resolved, which is not enough to determine both the gate and bias couplings. Note that the steep dashed lines (source-resonance) drawn in Fig. 1(c) do not allow for a reliable reading of the slope. However, the capacitances also enter in the slope of the broad NDC and PDC features inside the SET region, see blue line in Fig. 3(c), which in general are not parallel to the CNT diamond edges. As discussed below, these indicate a resonance between CNT and impurity orbitals. From these, we estimate $\alpha_g^i \approx 0.0055$ and $\alpha_s^i \approx 0.99$. The latter value indicates that the impurity level is "pinned" to the chemical potential of the source ($C_s \gg C_d, C_g$) and must therefore be localized much closer to this lead. For simplicity

we assume the CNT to be symmetrically coupled to the source and drain, $\Gamma_s^t = \Gamma_d^t$. (The general transport features are found not to change qualitatively if an asymmetry is introduced.) The impurity tunnel rates cannot be read off directly, but through an extensive theoretical survey we find that the best agreement with the experiment is for a source coupling of the order of the CNT tunnel coupling and a negligible drain coupling [$\Gamma_s^i = 4\Gamma_{s,d}^t$, $\Gamma_d^i = 0$ was used to obtain the result shown in Fig. 3(a)]. This is consistent with the above finding based on the capacitances that the impurity level is localized close to the source. The "top" of the impurity diamond is not clearly visible in Figs. 1(a) and 1(b). Nevertheless, judging from the guiding lines drawn in Fig. 1(c), we can estimate the impurity charging energy from the height of the smaller middle diamond to be $E_C^i \approx 2.5$ meV. The "impurity diamonds" in Fig. 1(c) show a distinct even-odd effect, indicating a large level-spacing, $\Delta E^i \approx 2.5$ meV, and we only include one impurity orbital in the model calculation. The hybridization between impurity and nanotube can be read off from the magnitude of the avoided crossing to be $t \approx 0.15$ meV.

Altogether, the agreement between the experiment, Fig. 2(a), and model calculation, Fig. 3(a), is striking. We now discuss and explain several qualitative features seen in both these plots. The unusual almost horizontal resonance line, passing through the Coulomb diamonds at positive bias, results in pronounced avoided crossings with the source SET resonance only [marked with white arrows in Fig. 2(a)]. At this point states with different numbers of electrons on the CNT and impurity hybridize strongly and the corresponding resonance lines avoid each other. Within the SET regime are broad regions of PDC and NDC extending from the avoided crossings. These are, in fact, further signatures of the resonant hybridization along the entire thick solid line sketched in Fig. 3(c). This mixing of impurity and tube states gives rise to interference terms in the tunnel rates, which in turn affect the conductance. Importantly, these conductance features do not correspond to the usual condition of a resonance between a dot and a lead chemical potential, but rather an internal resonance of the peapod system. The width of this resonance is set by the hybridization t and the tunnel rate asymmetry, rather than temperature or tunnel broadening. For the gate voltages we focus on here, none of the above features are seen at negative bias since, due to the impurity bias coupling, the states which anticross here are too high in energy to participate in transport. Instead, a regular pattern of sharp conductance lines are seen, as expected for a pure CNT system. The avoided crossings show an even-odd effect with alternating magnitude of the gap, e.g., the one in the large central diamond is less pronounced than those in the small neighboring diamonds. The reason is that a filled CNT subband hybridizes more strongly with an empty impurity state, as compared to the case where either one has an open shell. Furthermore, the impurity line does not pass straight through consecutive diamonds, but instead makes a small upward jump (when increasing V_g) between two diamonds. This implies a finite capacitive coupling between CNT and impurity states and therefore a "CNT—impurity charging energy," which we estimate as $E_C^{t-i} \approx 0.1$ meV, see Fig. 3(c). In contrast to standard SET, the low-bias magnitude of the impurity conductance lines depend sensitively on the voltages and in particular they become very weak far from the avoided crossing. This observation corroborates our earlier conclusion that the impurity is located near the source, and far away from the drain, which also implies that the impurity state is only tunnel coupled to the source and the resonance lines seen are due to tunneling from the drain. Only because of the hybridization with the CNT orbitals there is an effective voltage-dependent tunnel coupling to both leads, which becomes weaker further away from the avoided crossing. There are also higher lying resonances, as seen especially in the large central diamond and indicated in Fig. 3(c). The bias-voltage separation to the lower impurity resonance is equal to the subband splitting, $\delta = 1.2$ meV, and these higher lying impurity resonances therefore correspond to tunneling into the impurity, while at the same time the CNT is excited by transferring one electron to the higher subband. This is possible since the hybridization between the individual subbands and the impurity induces an effective coupling between the subbands.

IV. DISCUSSION

Having determined the properties of the impurity state and its coupling to the CNT, we now return to the question of its nature. One possibility is that we are dealing with an accidental impurity residing outside the tube. In fact, this would be somewhat similar to the alternative explanation given at the end of Ref. 20, where there were no fullerenes present. However, after the measurements presented above, the device was covered with PMMA and the center of the tube was suspended by electron beam lithography followed by wet etching in a buffered solution of hydrofluoric acid, creating an approximately 75 nm deep trench in the SiO_2 layer. The result of low-temperature transport spectroscopy measurements after suspension are shown in Fig. 2(b) and display features very similar to before suspension. Most importantly, the weakly gate-dependent impurity resonance is still present after suspension. It is clearly seen at both negative and positive bias in the gate-range shown in Fig. 2(b), allowing an estimate of roughly ~ 5 meV as an upper bound for its charging energy. Also the magnitude of the hybridization as well as the impurity tunnel couplings remain essentially unaltered by the etching process. This makes the scenario of an impurity outside the CNT less likely.

Another possibility would be that the impurity is in fact a segment of the CNT close to the source lead, separated from the rest of the tube by a local defect. However, our extensive model calculations clearly show that the transport data can only be reproduced if the CNT orbitals have a significant coupling to both source and drain leads, on the same order as the impurity-source tunnel coupling.

Although no compelling evidence can be claimed, we argue that the above observations suggest that the impurity is in fact a chain of C_{60} molecules inside the CNT, residing close to the source electrode (a single C_{60} would have a much larger charging energy). The close proximity to the source (and to some extent the surrounding nanotube) electrostatically shields this fullerene chain, resulting in the low gate coupling.

As mentioned above, some previous studies[4,8] have suggested tube-impurity hybridizations several orders of magnitude larger than the ~0.15 meV observed here. However, different studies predict very different hybridization strengths, which is also expected to depend sensitively on the type of peapod being measured. In the present case, the detailed transport analysis clearly shows that we are not dealing with a chain of fullerenes extending throughout the tube, but rather a limited chain close to one tube end. Additionally, the CNT is operated in the Coulomb blockade regime, where electron-electron interactions play a dominant role in determining the mixing of the CNT and impurity many-electron states.

In conclusion, we have measured low-temperature transport through a single-walled carbon nanotube peapod quantum dot. Anomalous weakly gate-dependent resonances, which show avoided crossings with the standard CNT Coulomb diamonds, originate from an impurity which is coupled both capacitively and by tunneling to its host nanotube. Such coupled quantum dot systems with different electrostatic properties can arise in various nanoscale transport junctions and the detailed study presented here is of general use for interpreting spectroscopic data. For instance the data in Ref. 21 show evidence of a similar weakly gated "impurity state" giving rise to NDC as it crosses the main diamond edge. Close inspection of the data in Ref. 11 also reveal features which may be interpreted in the same context. In the present case, several observations point at the impurity in fact being a chain of C_{60} molecules inside the nanotube, which is further supported by similar measured data in another peapod device. The experimental observation of electrically controlled mixing between the host nanotube and fullerenes is important since it opens up the possibility of using the latter's degrees of freedom for applications,[22] for instance via the induced spin-exchange coupling.

ACKNOWLEDGMENTS

This work was supported by the Danish Agency for Science, Technology and Innovation (J.P.), DFG-Forschergruppe 912 (S.S.), the European Union under the FP6 STREP program CANEL (A.E., J.N.), FP7 STREP program SINGLE (J.P., K.F., M.L.), and Grant No. DFG SPP-1243 (M.L., M.W.). We thank Pawel Utko and Laure Noé for experimental contributions.

*Author to whom correspondence should be addressed; paaske@fys.ku.dk

[1] B. W. Smith, M. Monthioux, and D. E. Luzzi, Nature (London) **396**, 323 (1998); M. Monthioux, Carbon **40**, 1809 (2002).
[2] S. Okada, S. Saito, and A. Oshiyama, Phys. Rev. Lett. **86**, 3835 (2001).
[3] C. L. Kane, E. J. Mele, A. T. Johnson, D. E. Luzzi, B. W. Smith, D. J. Hornbaker, and A. Yazdani, Phys. Rev. B **66**, 235423 (2002).
[4] J. Lu, S. Nagase, S. Zhang, and L. Peng, Phys. Rev. B **68**, 121402(R) (2003).
[5] Y.-G. Yoon, M. S. C. Mazzoni, and S. G. Louie, Appl. Phys. Lett. **83**, 5217 (2003).
[6] O. Dubay and G. Kresse, Phys. Rev. B **70**, 165424 (2004).
[7] H. Kondo, H. Kino, and T. Ohno, Phys. Rev. B **71**, 115413 (2005).
[8] D. J. Hornbaker, S.-J. Kahng, S. Misra, B. W. Smith, A. T. Johnson, E. J. Mele, D. E. Luzzi, and A. Yazdani, Science **295**, 828 (2002).
[9] H. Shiozawa, H. Ishii, H. Kihara, N. Sasaki, S. Nakamura, T. Yoshida, Y. Takayama, T. Miyahara, S. Suzuki, Y. Achiba, T. Kodama, M. Higashiguchi, X. Y. Chi, M. Nakatake, K. Shimada, H. Namatame, M. Taniguchi, and H. Kataura, Phys. Rev. B **73**, 075406 (2006).
[10] P. Utko, J. Nygård, M. Monthioux, and L. Noé, Appl. Phys. Lett. **89**, 233118 (2006).
[11] C. H. L. Quay, J. Cumings, S. J. Gamble, A. Yazdani, H. Kataura, and D. Goldhaber-Gordon, Phys. Rev. B **76**, 073404 (2007).
[12] H. Y. Yu, D. S. Lee, S. H. Lee, S. S. Kim, S. W. Lee, Y. W. Park, U. Dettlaff-Weglikowskaand, and S. Roth, Appl. Phys. Lett. **87**, 163118 (2005).
[13] J. Mizubayashi, J. Haruyama, I. Takesue, T. Okazaki, H. Shinohara, Y. Harada, and Y. Awano, Phys. Rev. B **75**, 205431 (2007).
[14] M. R. Buitelaar, A. Bachtold, T. Nussbaumer, M. Iqbal, and C. Schönenberger, Phys. Rev. Lett. **88**, 156801 (2002).
[15] W. Liang, M. Bockrath, and H. Park, Phys. Rev. Lett. **88**, 126801 (2002).
[16] S. Sapmaz, P. Jarillo-Herrero, J. Kong, C. Dekker, L. P. Kouwenhoven, and H. S. J. van der Zant, Phys. Rev. B **71**, 153402 (2005).
[17] L. Mayrhofer and M. Grifoni, Eur. Phys. J. B **63**, 43 (2008).
[18] H. Bruus and K. Flensberg, *Many-Body Quantum Theory in Condensed Matter Physics* (Oxford University Press, New York, 2004).
[19] S. De Franceschi, S. Sasaki, J. M. Elzerman, W. G. van der Wiel, S. Tarucha, and L. P. Kouwenhoven, Phys. Rev. Lett. **86**, 878 (2001).
[20] A. K. Hüttel, B. Witkamp, M. Leijnse, M. R. Wegewijs, and H. S. J. van der Zant, Phys. Rev. Lett. **102**, 225501 (2009).
[21] E. A. Osorio, K. O'Neill, M. R. Wegewijs, N. Stuhr-Hansen, J. Paaske, T. Bjørnholm, and H. S. J. van der Zant, Nano Lett. **7**, 3336 (2007).
[22] S. C. Benjamin, A. Ardavan, G. A. D. Briggs, D. A. Britz, D. Gunlycke, J. Jefferson, M. A. G. Jones, D. F. Leigh, B. W. Lovett, A. N. Khlobystov, S. A. Lyon, J. J. L. Morton, K. Porfyrakis, M. R. Sambrook, and A. M. Tyryshkin, J. Phys.: Condens. Matter **18**, S867 (2006).